INSTITUTE OF PHYSICS PUBLISHING JOURNAL OF PHYSICS: CONDENSED MATTER

J. Phys.: Condens. Matter **17** (2005) S2641–S2656 doi:10.1088/0953-8984/17/24/018

Granular gases in compartmentalized systems

Umberto Marini Bettolo Marconi[1], **Giulio Costantini and Daniela Paolotti**

Dipartimento di Fisica, Università di Camerino and Istituto Nazionale di Fisica della Materia, Via Madonna delle Carceri, 62032, Camerino, Italy

E-mail: umberto.marinibettolo@unicam.it

Received 16 March 2005
Published 3 June 2005
Online at stacks.iop.org/JPhysCM/17/S2641

Abstract

This contribution considers recent developments in understanding the behaviour of vibro-fluidized beads in containers partitioned into several connected chambers. The system is studied theoretically by means of a phenomenological mean-field approach. The equations governing the evolution of the average occupancy and the average kinetic energy of each compartment are derived by means of a simplified treatment of the Boltzmann equation.

Some applications of the method are presented. These include the study of a simple granular gas in a many-compartment container and a binary granular mixture in a two-compartment container.

(Some figures in this article are in colour only in the electronic version)

1. Introduction

The study of the properties of granular gases, i.e. rarefied systems of macroscopic particles mutually interacting by strongly repulsive and dissipative forces, is currently a subject of great interest for a variety of reasons which range from technological applications, including grain separation and jam formation, to fundamental issues for the statistical mechanics of systems far from equilibrium [1–4]. A vibro-fluidized granular gas is a dilute collection of grains set in motion by a tapping or shaking mechanism, which balances the energy dissipated by the inelastic collisions. The steady state properties of such a system display interesting analogies with those of standard molecular fluids, but also display original features. One of these features is the spontaneous tendency of the particles to form clusters. Uniformity and homogeneity of large assemblies of fluidized grains are the exception rather than the rule. That is for two main reasons: (a) the walls of the containers represent a strong perturbation; (b) the homogeneous state is intrinsically unstable, and velocity and density correlations lead to the appearance of vortices and clusters [5–8].

[1] Author to whom any correspondence should be addressed.

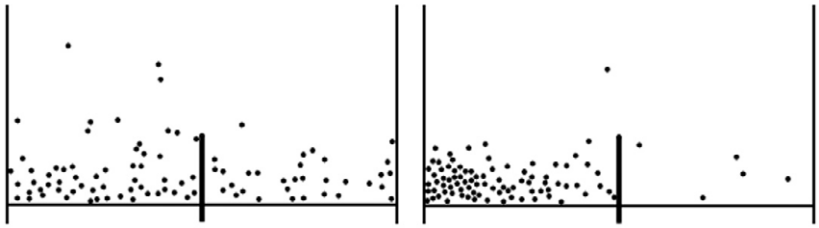

Figure 1. Sand demon in a two-compartment system. The left picture shows a symmetric configuration obtained when the grains are subjected to a strong driving force, while the right picture represents an instance of an asymmetric configuration which occurs for a weaker driving intensity.

In a pioneering experiment, Nordmeier and Schlichting [9] have shown that a collection of grains vigorously agitated in a two-compartment vessel (the compartments being connected by a hole located at a certain height from the bottom vibrating base) can visit all regions of the container. As a consequence, the populations in the two compartments are statistically equal. The situation changes when the amplitude of the vibrations decreases below a certain critical value. In fact, when the largest altitude reached by the particles is comparable with the elevation of the hole, one observes a separation process where a minority of 'hot' quickly moving particles migrates to one side, while the majority of 'cold' slowly moving particles spontaneously condenses on the other side, as shown in figure 1. The asymmetry increases as the vibration intensity decreases. The feature that the particles in the scarcely occupied compartment are on the average faster than the others has motivated the name 'Maxwell's demon made of sand' given to the experiment, in analogy with the hypothetical being who looks at gas molecules, and depending on their speeds opens or closes a door collecting all the molecules faster than average on one side, and the slower ones on the other side.

Notwithstanding this spectacular effect, the phenomenon possesses a simple qualitative explanation and the second law of thermodynamics is not violated, since the grains can adsorb and dissipate energy unlike the molecules of an ideal gas. When the driving is sufficiently low, the uniform state is unstable since to a local density increase there corresponds a decrease in the local kinetic energy, which causes fewer particles to flow away from such a region. Eventually, a stationary state is reached where few grains remain on one side and undergo few collisions, while the remaining congregate on the other side a form a colder and denser cluster. Eggers has explained the origin of the phenomenon using a hydrodynamic theory [10] known as the Flux model, which has been extended by the Twente group [11–13], in order to analyse situations where more than two compartments were involved.

Later, Lipowski and Droz [14, 15] have elaborated a generalization of the Ehrenfest urn model [16], which could be treated with the standard tools of statistical mechanics such as a master equation approach or Monte Carlo simulation and has the advantage of being simple enough to allow a great deal of analytical calculations and extensive numerical computations. In the simplest version of their model, N particles are distributed between two urns. Each particle can jump from one urn to the other with a probability which decreases as the number of particles in the former increases. Thus the exchange rate depends only on the number of particles at the departure site and not on the number of particles at the arrival site. With respect to such a property, the model is similar to a zero range process [17, 18]. When the energy dissipated is sufficiently large with respect to the energy injected, a spontaneous symmetry breaking takes place. Due to its great simplicity, the model allows for a great deal of analytic work. However, the extension of such 'minimal' models to more than one component where

each species has its own temperature is quite problematic. Therefore, it is necessary to consider in some detail the microscopic dynamics of the grains. Kinetic theory has also been applied to the problem of two compartments by Brey and co-workers [19], while a coarse-grained version of the kinetic approach was employed in [20–22].

The present paper is organized as follows. In the first section we define the model and introduce the statistical description of the system, based on a Boltzmann equation for the distribution functions, modified to take into account the stochastic driving and the presence of the compartments. At this stage we follow the strategy of integrating out microscopic fluctuations going from a microscopic description based on the Boltzmann equation to a macroscopic level, where only the occupation numbers and the granular temperatures of the compartments, i.e. the first two moments of the distribution function, are taken into account. This is equivalent to neglecting inhomogeneities of the system at scales smaller than the linear size of the compartments. By means of a simplifying ansatz for the velocity distribution function we obtain a closed set of self-consistent differential equations for the occupation numbers and the granular temperatures of the two compartments.

We discuss in some detail some selected applications of the method including a simple granular gas in two compartments and in many compartments, and a binary mixture in two compartments. In each case a linear stability analysis is performed, together with the numerical solution of the non-linear coupled differential equations, and the relevant behaviours are shown.

2. Model

We consider an assembly of $\mathcal{N}$ inelastic hard spheres moving in a two-dimensional domain partitioned into M identical regions of volume, V separated by vertical obstacles. Each compartment contains N_i particles, where $\sum_{i=1}^{M} N_i = \mathcal{N}$, and belongs to a one-dimensional array.

The velocities after the collision, denoted with a prime, are obtained in terms of the (unprimed) pre-collisional velocities through the relations

$$\begin{aligned} \mathbf{v}_1' &= \mathbf{v}_1 - \tfrac{1}{2}(1+\alpha)(\mathbf{v}_{12}\cdot\hat{\boldsymbol{\sigma}})\hat{\boldsymbol{\sigma}}, \\ \mathbf{v}_2' &= \mathbf{v}_2 + \tfrac{1}{2}(1+\alpha)(\mathbf{v}_{12}\cdot\hat{\boldsymbol{\sigma}})\hat{\boldsymbol{\sigma}} \end{aligned} \quad , \tag{1}$$

where $\mathbf{v}_{12} = \mathbf{v}_1 - \mathbf{v}_2$, $\hat{\boldsymbol{\sigma}}$ is the unit vector directed from particle 1 to particle 2, and α is the coefficient of restitution. The rate at which the kinetic energy is dissipated by collisions is proportional to $(1-\alpha^2)$.

A particle in the ith box, besides colliding inelastically with the remaining $(N_i - 1)$ particles within the same box, is subjected to the action of a white noise random force, which compensates the energy losses due to dissipative forces and stands for the external driving force.

The dynamics of the kth particle between two successive collisions is governed by the Langevin equation

$$\frac{\mathrm{d}\mathbf{v}_k}{\mathrm{d}t} = -\frac{1}{\tau_b}\mathbf{v}_k + \boldsymbol{\xi}_{\mathbf{k}}, \tag{2}$$

where $-\tau_b^{-1}\mathbf{v}_k$ is a viscous term and $\xi_{\mathbf{k}}$ a Gaussian random acceleration, whose average is zero, and the variance satisfies a fluctuation-dissipation relation:

$$\langle \xi_{k\mu}(t)\xi_{m\nu}(t')\rangle = 2\frac{T_b}{m\tau_b}\delta_{km}\delta_{\mu\nu}\delta(t-t'), \tag{3}$$

where T_b is proportional to the intensity of the driving [23] and μ, ν denote vector components. The damping term renders the system stationary even in the absence of collisional dissipation and physically represents the friction between the particles and the container.

Finally, the particles contained in compartment i can migrate into a nearest neighbour compartment j with a probability per unit time τ_s^{-1}, provided their kinetic energy exceeds the fixed threshold T_s.

The single-particle phase-space distribution function $f(\mathbf{r}, \mathbf{v}, t)$ for such a system can be obtained by solving the associated inhomogeneous Boltzmann equation. However, by resorting to the coarse graining approximation,

$$f(\mathbf{r}, \mathbf{v}, t) = f_i(\mathbf{v}, t) \tag{4}$$

which is equivalent to replacing the dependence on the continuous variable $\mathbf{r}$ with a discrete index i indicating the compartment where the point $\mathbf{r}$ is located, one obtains a much simpler description. Within such an approximation one finds the following Boltzmann-like equation:

$$\partial_t f_i(\mathbf{v}, t) = I[\mathbf{v}|f_i, f_i] + \mathcal{B} f_i + \mathcal{X}[\mathbf{v}|f_i, f_j], \tag{5}$$

where the three terms on the right-hand side represent different physical mechanisms.

The first term, I, is the collision term which describes the effect of inelastic collisions among particles belonging to the same compartment, $\mathcal{B} f_i$ represents the action of the stochastic driving force associated to the heat bath, and $\mathcal{X}[f_i, f_j]$ represents the flow between two adjacent compartments.

Within Boltzmann's chaos hypothesis, the integral I has the following representation:

$$I[\mathbf{v}_1|f_i, f_i] = \sigma \int \mathrm{d}\mathbf{v}_2 \int \mathrm{d}\hat{\boldsymbol{\sigma}}\, \theta(\hat{\boldsymbol{\sigma}} \cdot \mathbf{v}_{12})(\hat{\boldsymbol{\sigma}} \cdot \mathbf{v}_{12}) \left[\frac{1}{\alpha^2} f_i(\mathbf{v}_1'') f_i(\mathbf{v}_2'') - f_i(\mathbf{v}_1) f_i(\mathbf{v}_2) \right]. \tag{6}$$

θ is the Heaviside step function, doubly primed symbols stand for pre-collisional velocities, which can be computed by inverting equation (1), and the α^2 factor in the denominator incorporates the effect of inelasticity.

The forcing term assumes the form

$$\mathcal{B} f_i(\mathbf{v}, t) = \frac{1}{\tau_b} \frac{\partial}{\partial \mathbf{v}} \left(\frac{T_b}{m} \frac{\partial}{\partial \mathbf{v}} + \mathbf{v} \right) f_i(\mathbf{v}, t), \tag{7}$$

while the exchange term can be written as

$$\mathcal{X}[\mathbf{v}|f_i, f_j] = -\frac{1}{\tau_s} \theta(|\mathbf{v}| - u_s) \sum_j{}' [f_i(\mathbf{v}, t) - f_j(\mathbf{v}, t)], \tag{8}$$

where u_s is the threshold velocity and the primed summation includes only the nearest neighbours j of the site i.

To proceed further we consider the macro-state of the system, which can be characterized by the average number, $N_i(t)$, of particles occupying each compartment i at time t,

$$N_i(t) = \int \mathrm{d}\mathbf{r} \int \mathrm{d}\mathbf{v}\, f_i(\mathbf{v}, t), \tag{9}$$

and by the average kinetic energy (granular temperature), $T_i(t)$, in each compartment:

$$N_i(t) T_i(t) = \int \mathrm{d}\mathbf{r} \int \mathrm{d}\mathbf{v}\, \frac{m v^2}{2} f_i(\mathbf{v}, t). \tag{10}$$

Using equation (5) one finds

$$\frac{\mathrm{d}N_i(t)}{\mathrm{d}t} = -\frac{V}{\tau_s} \sum_j{}' \int \mathrm{d}\mathbf{v}\, [f_i(\mathbf{v}, t) - f_j(\mathbf{v}, t)] \theta(|\mathbf{v}| - u_s) \tag{11}$$

and

$$\frac{1}{V}\partial_t(N_i T_i) = \frac{m}{2}\int \mathrm{d}\mathbf{v}\, v^2 I[\mathbf{v}|f_i, f_i] + \frac{m}{2}\int \mathrm{d}\mathbf{v}\, v^2 \mathcal{B} f_i - \frac{m}{2\tau_s}\sum_j{}' \int \mathrm{d}\mathbf{v}\, v^2 [f_i(\mathbf{v},t) - f_j(\mathbf{v},t)]\theta(|\mathbf{v}| - u_s). \tag{12}$$

In two dimensions, one can obtain a closed set of equations if one makes the following Maxwell–Boltzmann (MB) approximation for the velocity distribution functions in each compartment:

$$f_i(\mathbf{v},t) = \frac{N_i(t)}{V}\frac{m}{2\pi T_i(t)}\exp\left(-\frac{m\mathbf{v}^2}{2T_i(t)}\right). \tag{13}$$

The assumed MB form is not necessary, but it is very convenient to make analytical progress. On the other hand, to improve the present approximation, one could express the velocity distribution as an MB distribution multiplied by a linear combination of orthogonal polynomials, called Sonine polynomials [24]. This modification would allow us to include the effect of fluctuations around the MB distribution, but for the sake of simplicity we shall not pursue such a route.

In this case, $N_i(t)$ and $T_i(t)$ can be determined self-consistently by solving the following governing equations, which are obtained by inserting equation (13) into (11) and (12):

$$\frac{\mathrm{d}N_i(t)}{\mathrm{d}t} = \frac{1}{\tau_s}[N_{i+1}\mathrm{e}^{-T_s/T_{i+1}} + N_{i-1}\mathrm{e}^{-T_s/T_{i-1}} - 2N_i\mathrm{e}^{-T_s/T_i}] \tag{14}$$

and

$$N_i\frac{\mathrm{d}T_i(t)}{\mathrm{d}t} = \frac{1}{\tau_s}[2(N_{i+1}T_{i+1}\mathrm{e}^{-T_s/T_{i+1}} + N_{i-1}T_{i-1}\mathrm{e}^{-T_s/T_{i-1}} - 2N_iT_i\mathrm{e}^{-T_s/T_i}) + (N_{i+1}\mathrm{e}^{-T_s/T_{i+1}} + N_{i-1}\mathrm{e}^{-T_s/T_{i-1}} - 2N_i\mathrm{e}^{-T_s/T_i})(2T_s - T_i)] - 2\gamma\omega_i N_i T_i + \frac{2}{\tau_b}N_i(T_b - T_i), \tag{15}$$

where the dissipation rate [24]

$$\gamma\omega_i = \sigma(1-\alpha^2)\frac{N_i}{2V}\sqrt{\frac{T_i}{m}} \tag{16}$$

stems from the collision integral and σ is the hard-disc diameter.

When the rate of exchange of particles between two adjacent compartments is low, one can approximate the granular temperature, $T_i(t)$, by a local function of the instantaneous value of the number of particles $N_i(t)$. This temperature is the solution of the non-linear equation:

$$T_i\left[1 + \tau_b\sigma(1-\alpha^2)\frac{N_i}{2V}\sqrt{\frac{T_i}{m}}\right] = T_b. \tag{17}$$

By substituting $T_i(t)$ in equation (14), the governing law of the system takes the simpler form:

$$\frac{\mathrm{d}N_i(t)}{\mathrm{d}t} = \frac{1}{\tau_s}[\Phi(N_{i+1}) + \Phi(N_{i-1}) - 2\Phi(N_i)], \tag{18}$$

where $\Phi(N)$ is depicted in figure 2. Equation (18) has the same form as the one which is at the heart of the so-called Flux model [12]. We notice that the detailed shapes of Φ in the Flux model and in our model are not identical, because they have been derived from different assumptions. However, the two models share the same non-monotonic behaviour of Φ as a function of N. This is sufficient to give similar qualitative results. In the sub-critical region, the existence

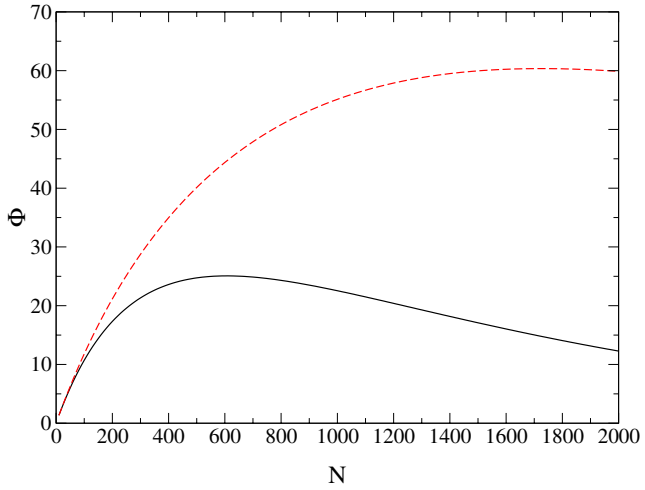

Figure 2. Flux function versus particle number for two different values of the heat bath temperature. The dashed curve represents a supercritical case, where the function is monotonically increasing as a function of the number of particles considered. The continuous curve, instead, describes a situation where due to the presence of a maximum there can be a balance of fluxes from unequally populated compartments.

of multiple roots of the non-linear equation $\Phi(N) = \text{constant}$ (see figure 2), corresponds to stationary solutions of the coupled equations (18) with N_i not necessarily the same in each cell. In other words, the flux from a relatively empty compartment can be balanced by the flux from a well filled compartment.

3. One species in two compartments

In the present section we illustrate the simplest application of the formalism above. Let us consider only two compartments, named A and B, and non-periodic boundary conditions, which mean that the exchange of energy and matter occurs only through the central dividing barrier. In this case we write

$$\frac{\mathrm{d}N_A(t)}{\mathrm{d}t} = \frac{1}{\tau_s}[N_B \mathrm{e}^{-T_s/T_B} - N_A \mathrm{e}^{-T_s/T_A}] \tag{19}$$

$$\frac{\mathrm{d}[N_A(t)T_A(t)]}{\mathrm{d}t} = -\frac{2}{\tau_s}[N_A(T_A+T_S)\mathrm{e}^{-T_s/T_A} - N_B(T_B+T_S)\mathrm{e}^{-T_s/T_B}] - 2\gamma\omega_A N_A T_A + \frac{2}{\tau_b}N_A(T_b - T_A) \tag{20}$$

$$\frac{\mathrm{d}[N_B(t)T_B(t)]}{\mathrm{d}t} = -\frac{2}{\tau_s}[N_B(T_B+T_S)\mathrm{e}^{-T_s/T_B} - N_A(T_A+T_S)\mathrm{e}^{-T_s/T_A}] - 2\gamma\omega_B N_B T_B + \frac{2}{\tau_b}N_B(T_b - T_B). \tag{21}$$

The choice $N_A = N_B = N^* = N/2$ and $T_A = T_B = T^*$ represents a stationary solution of equations (19)–(21) for all values of the control parameters. The temperature T^* is given by the non-linear equation:

$$T^*\left[1 + \tau_b\sigma(1-\alpha^2)\frac{N^*}{2V}\sqrt{\frac{T^*}{m}}\right] = T_b. \tag{22}$$

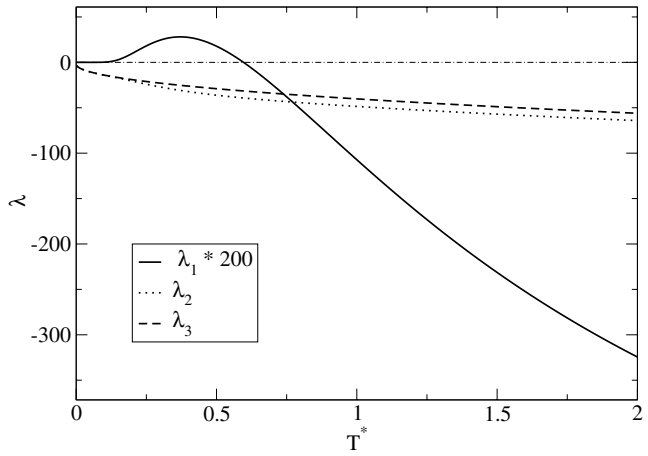

Figure 3. Variation of the eigenvalues $\lambda_1, \lambda_2, \lambda_3$ with respect to the granular temperature. Notice the temperature interval where λ_1 is positive and the symmetric configuration is unstable with respect to clustering.

On the other hand, such a symmetric solution is unstable below a certain temperature. This can be determined by performing a linear stability analysis, that is, assuming $T_A = T^* + \delta T_A$, $T_B = T^* + \delta T_B$ and $N_A = N^* + \delta N_A$ ($\delta N_B = -\delta N_A$) and expanding the equations to first order about the fixed point T^*, N^*. The resulting three relaxation modes are characterized by eigenvalues $\lambda_1 > \lambda_2 > \lambda_3$. In figure 3 we sketch the temperature dependence of the eigenvalues of the dynamical matrix.

Only λ_1 is relevant to our analysis. Its sign becomes positive below a special temperature $T^*_{\rm cr}$, determined by the condition $\lambda_1 = 0$, indicating that the symmetric solution becomes unstable. Such a regime corresponds to the non-symmetric solutions which are observed for weak external drive. The value of $T^*_{\rm cr}$ depends on the inelasticity and the particle density for a fixed value of the external driving intensity. When the system becomes perfectly elastic ($\alpha = 1$, $T^*_{\rm cr} \to 0$), since there is no clustering instability in a system of elastic particles.

In the case of unequally populated compartments the asymptotic ($t \to \infty$) values of the numbers of particles in the two compartments are related by the equation

$$\frac{N_B}{N_A} = \frac{{\rm e}^{-T_s/T_A}}{{\rm e}^{-T_s/T_B}}, \tag{23}$$

where the two granular temperatures are determined by the condition that the granular temperature at the right and the one at the left are constant solutions of equations (20) and (21).

The full time-dependent solutions of equations (19)–(21) have been obtained numerically by an Euler integration scheme and are displayed in figure 4, illustrating three different regimes.

For temperatures below $T^*_{\rm cr}$ the perturbation initially grows at an exponential rate $\exp(\lambda_1 t)$, as predicted by the previous linear stability analysis, and saturates asymptotically at a finite value. The resulting 'phase diagram' is shown in figure 5.

The above results can be compared with those of other groups. The experiments [13] seem to indicate that the separation process occurs continuously in a two-compartment set-up and discontinuously with three or more compartments. The two-urn model [14], in addition to having a line of continuous transitions, has a tricritical point and a line of discontinuous transitions. The discontinuous transitions are difficult to observe due to the strong metastability. The model we have considered presents the same features as the two-urn model.

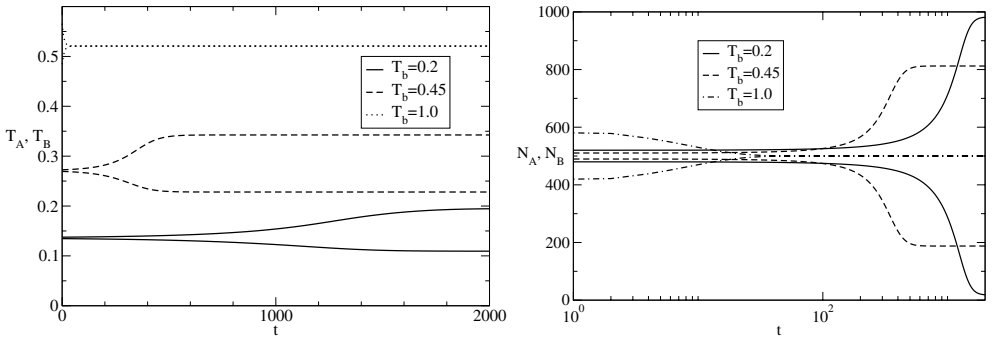

Figure 4. Two-compartment system. Left figure: evolution of the granular temperature in each compartment. The three cases correspond to three different values of the heat bath temperature. The two lower cases represent symmetry breaking situations, the upper curve (dotted line) represents a symmetric situation. Right figure: temporal evolution of the populations in the two compartments. The two non-symmetric solutions (continuous and dashed) correspond to subcritical cases, whereas the symmetric solution corresponds to a supercritical case.

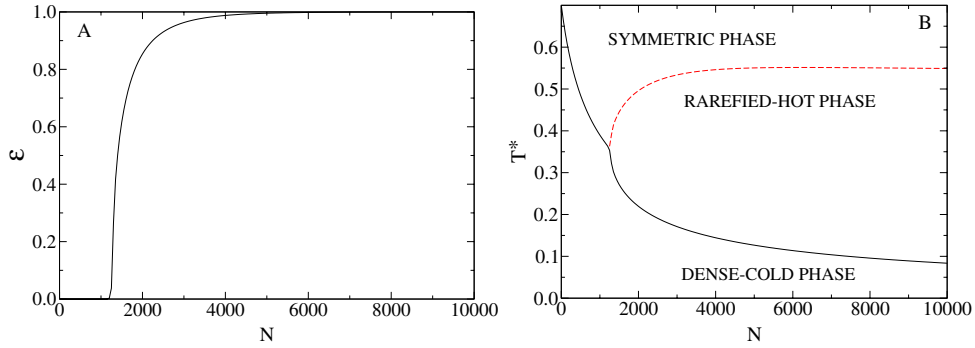

Figure 5. Two-compartment system. Order parameter $\epsilon = |N_A - N_B|/N$ versus total number of particles in the system N, and granular temperature of each compartment versus N. Notice the bifurcation of the temperature curve, corresponding to the symmetry breaking.

4. One species in many compartments

The case of $\mathcal{N}$ particles in M identical compartments with cyclic boundary conditions has been studied by in [12, 13, 21]. A uniform solution of equations (14) and (15) is represented by $N_i = N^* = \mathcal{N}/M$ and $T_i = T^*$, where T^* is a function of N^* (via equation (17)). Such a solution exists for all values of the control parameters, but is stable only at high temperatures. In analogy with the two-compartment case, the translational symmetry is broken at low temperatures of the driving heat bath. To show that, let us introduce a small sinusoidal perturbation about the uniform state: $T_l = T^* + \delta T_k \exp(\mathrm{i}kl)$, and $N_l = N^* + \delta N_k \exp(\mathrm{i}kl)$, where $k = 2\pi n/M$, with $n = 1, \ldots, M-1$ and $l = 1, \ldots, M$ denotes the compartment.

Expanding linearly equations (14) and (15) about the symmetric fixed point T^*, N^*, one finds the equations:

$$\delta\dot{N}_k = -\frac{1}{\tau_s}\mathrm{e}^{-T_s/T^*}2(1-\cos(k))\left[\delta N_k + \frac{N^* T_s}{(T^*)^2}\delta T_k\right] \tag{24}$$

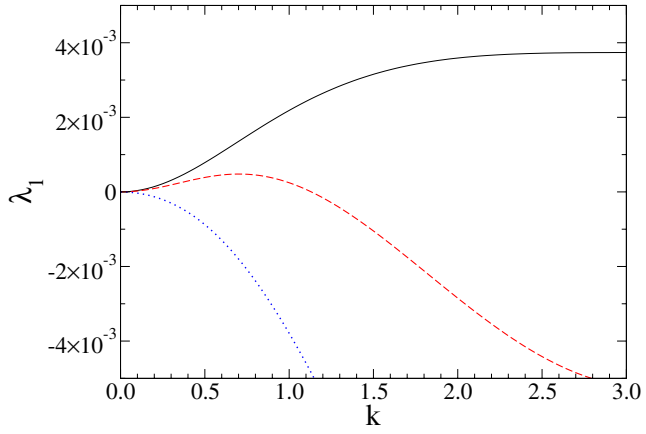

Figure 6. Three possible behaviours of the eigenvalue $\lambda_1(k)$ relative to the many-compartment system. The two upper curves refer to weak driving situations where the uniform profile is unstable with respect to density fluctuations.

$$\delta\dot{T}_k = -\frac{1}{\tau_s}\mathrm{e}^{-T_s/T^*}\left[\left(2+\frac{T_s}{T^*}+2\left(\frac{T_s}{T^*}\right)^2\right)(1-\cos(k))+\left(3\gamma\omega^*+\frac{2}{\tau_b}\right)\right]\delta T_k$$
$$-\frac{2}{N^*}\left[\frac{1}{\tau_s}\mathrm{e}^{-T_s/T^*}(T^*+2T_s)(1-\cos(k))+\gamma\omega^*T^*\right]\delta N_k. \tag{25}$$

In this case, one finds two families of eigenvalues $\lambda_1(k)$ and $\lambda_2(k)$, a pair for each value of k, corresponding to the two relaxation modes of the system. The larger eigenvalue $\lambda_1(k)$ vanishes quadratically in the limit $k \to 0$, due to the conservation of the total number of particles, and displays a non-trivial behaviour for finite values of k, which is captured by the following small-k expansion:

$$\lambda_1(k) = a_2k^2 + a_4k^4, \tag{26}$$

where the coefficient a_2 is given by the formula

$$a_2 = \frac{1}{\tau_s}\mathrm{e}^{-T_s/T^*}\left[\frac{T_c}{T^*}-1\right] \tag{27}$$

and becomes positive below the temperature T_c:

$$T_c = \frac{T_s}{\frac{3}{2}+\frac{1}{\tau_b\gamma\omega^*}}. \tag{28}$$

Above T_c, a_2 is negative, and a local density fluctuation is re-absorbed.

In contrast, below T_c a fluctuation, which locally increases the population, is amplified and clustering occurs. The local granular temperature, T_i, drops due to the increased collision rate, since from equation (16) one sees that $\omega_i \propto N_iT_i^{1/2} \propto N_i^{2/3}$, being $T_i \propto N_i^{-2/3}$. Thus the particles arriving from the other compartments remain trapped, causing a further reduction of the local temperature.

According to the sign of a_4 (for $a_2 > 0$) one observes different initial regimes: if $a_4 < 0$, $\lambda_1(k)$ may display a maximum at a finite wavevector, $k_m < 2\pi$, whereas for $a_4 > 0$, $\lambda_1(k)$ attains its maximum only in correspondence of the largest wavevector as displayed in figure 6. In the first case, associated with the dashed curve in figure 7 ($a_2 > 0$ and $a_4 < 0$), there is a fastest growing wavelength at early times. Thus the process resembles the early stage of

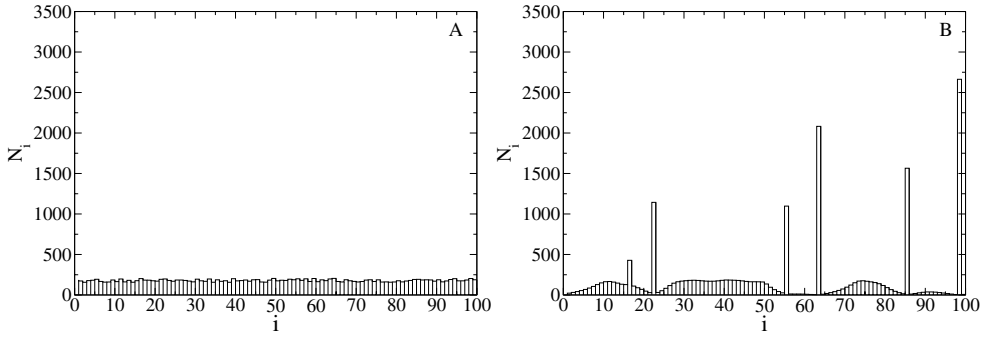

Figure 7. Coarsening process in the low-temperature phase. The initial nearly uniform profile becomes unstable and the population of a few compartments grows at the expense of the others. Picture A refers to an early stage, and B to a late stage.

spinodal decomposition, because the homogeneous state is unstable and all modulations of the order parameter with k such that $\lambda_1(k) > 0$ grow, but the maximum growing rate corresponds to the maximum of the dashed curve in figure 7 [25].

To study the late-stage behaviour of the solutions one has to go beyond the linear stability analysis. This is achieved by solving numerically the governing non-linear equations (14) and (15). The asymptotic solution may depend on the initial state. In [21] a one-dimensional array of compartments, initially equally populated, at the same granular temperature, i.e. $N_i = N^*$ and $T_i = T^*$, plus a small random perturbation was considered, and different behaviours were observed as some control parameters, such as the heat bath temperature and the average density, were varied. For $T_i > T_c$, the initial perturbation is re-adsorbed diffusively, while below T_c the perturbation is exponentially amplified in the initial stage. In the latter case, the collisional cooling determines a decrease of the local temperature in correspondence of the more populated regions, and clustering begins. Some compartments, randomly selected by the dynamics, act as germs for the nucleation process illustrated in figure 7. After the initial regime a few compartments grow at the expense of the remaining ones, which become empty. We observe that the domains do not grow in width, but in height, with a law $N(t) \sim t^{1/2}$, and they do not merge.

Clustering has been measured by defining a statistical indicator, with the property of vanishing when all particles are confined in a single compartment and of taking its maximum value, $\ln(M)$, when all compartments are identically populated:

$$h = -\sum_i^M \frac{N_i}{\mathcal{N}} \ln\left(\frac{N_i}{\mathcal{N}}\right). \tag{29}$$

In pictorial language $f = \exp(h)$ represents the number of occupied compartments. Above T_c, f relaxes towards M, meaning that all compartments are occupied, whereas in the low temperature region f settles at a value $P < M$, meaning that only a few compartments are effectively filled. To characterize such a process we consider the characteristic time τ necessary to grow a domain, i.e. to have $f \ll M$, starting from a nearly homogeneous configuration. Such a time τ depends on the temperature, and as T^* approaches T_c from below, its variation, displayed in figure 8, is captured by the following Vogel–Fulcher law:

$$\tau = A \exp[\Delta/(T_c - T^*)], \tag{30}$$

where Δ is a constant. The dependence of the characteristic time τ on the temperature is a direct consequence of the functional dependence of a_2 on the temperature (see equations (26) and (27)).

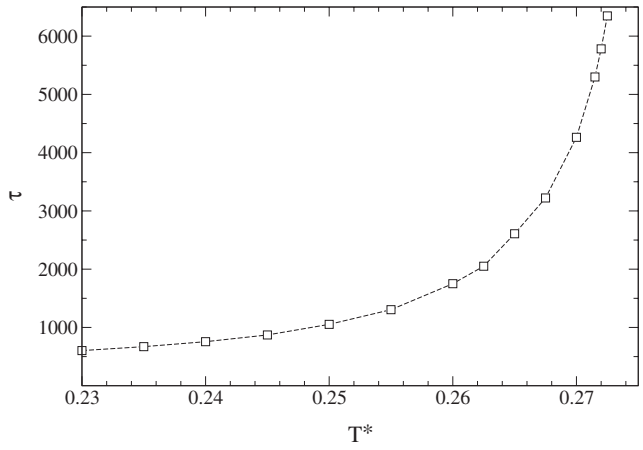

Figure 8. Time, τ, which characterizes the clustering of the granular gas in a single compartment as a function of the temperature, starting from an array of $M = 100$ compartments equally populated.

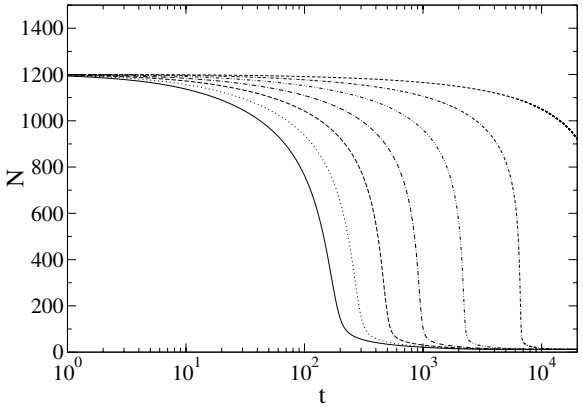

Figure 9. Variation of the height of a cluster, initially containing 1200 particles, as a function of time for temperatures $T_b = 0.30$, 0.35, 0.40, 0.45, 0.50, 0.55 and 0.60 from top to bottom.

A different phenomenon, which has recently attracted some attention [12], is the sudden collapse of a granular cluster. Experiments show that a configuration in which the majority of the grains are located in a single compartment remains stable for a long time until the grains suddenly leave the compartment and diffuse through the system.

Within the present approach, according to the noise intensity of T_b one can observe two different relaxation processes: (a) for large T_b the occupancy of the compartment decays towards the fully symmetric state $N_i = \mathcal{N}/M$; (b) for small T_b the occupancy of the compartment remains constant.

In figure 9 we display how the occupancy of an initially filled compartment evolves in correspondence of various values of the heat bath temperature. We observe that $N(t)$ decreases more and more slowly as the transition temperature is approached from above. Figure 9 also shows the appearance of a plateau when $T_b \to T_0$, whose length diverges at T_0. Below the temperature T_0 the cluster is stable. Numerical calculations show that the persistence time τ of the single-cluster configuration can be described by $\tau = C/(T_b - T_0)^{3/2}$, which diverges at the crossover temperature T_0, which is a function of the system size and of the cluster height.

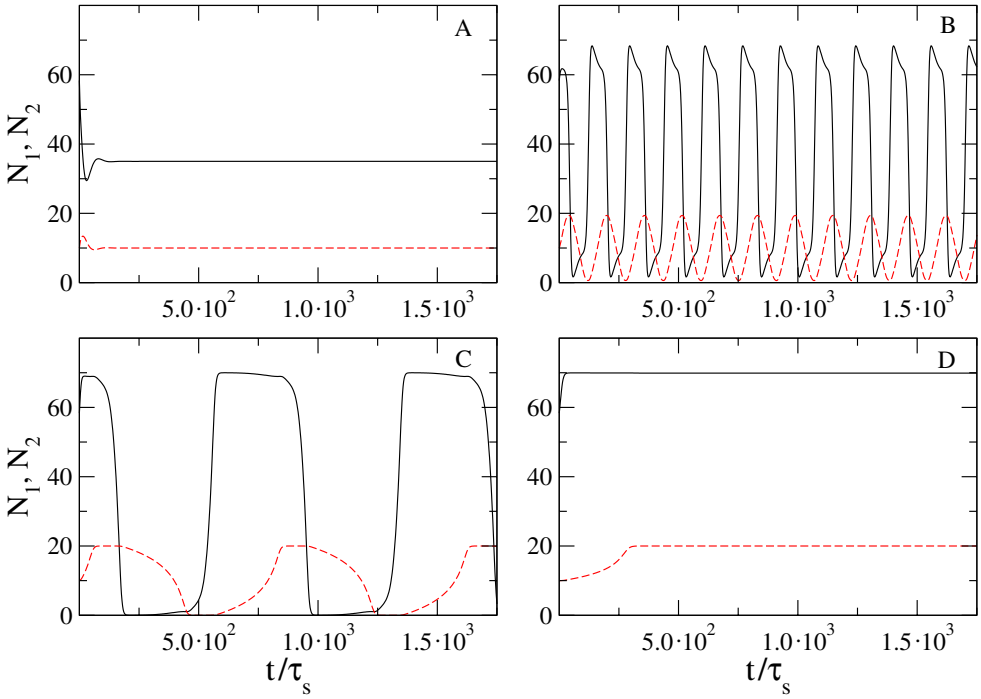

Figure 10. Four different behaviours obtained by varying the dimensionless parameter $R_{\rm MF}$, and keeping the mass ratio $m_2/m_1 = 8$ and the population ratio $N_1/N_2 = 70/20$. The continuous line (N_1) refers to the light species and the dotted line (N_2) to the heavy species, both in the right compartment. In panel A ($R_{\rm MF} = 6.0$) the asymptotic solution is symmetric. In panel B ($R_{\rm MF} = 12$) the occupation numbers oscillate in time. Panel C ($R_{\rm MF} = 24$) shows a case where the solution displays oscillations with longer periods. Finally, panel D ($R_{\rm MF} = 48$) illustrates a typical symmetry-breaking solution, where occupation numbers in the two compartments are different, for each species. The time is measured in units τ_s.

5. Mixture in two compartments

In the present section we shall briefly discuss the effect of bi-dispersity into the system. Mikkelsen *et al* [26] have studied experimentally the behaviour of a bi-disperse granular mixture of small and large particles in a compartmentalized geometry, and they showed that the system has a tendency to cluster competitively.

The mean-field treatment employed in the previous sections has been extended to mixtures of grains of different sizes and/or masses [22]. In this case, the macro-state of the system was identified by two occupation numbers, one for each species, and by four granular temperatures, one for each species and each compartment. Again, for strong driving only a symmetric configuration, characterized by equal values of the state variables in the two compartments, was found. However, for small driving intensity or high dissipation the configuration ceases to be symmetric, and the particles of both species tend to cluster in one of the two compartments in agreement with the experimental observations. In figure 10 we show the temporal evolution of occupation numbers for the two species (in a single compartment) for different choices of the driving intensity. We observe two dynamical scenarios. In the first scenario, the occupation numbers approach a stationary symmetry-broken solution via a simple bifurcation (i.e. a critical point). This corresponds to the situation considered in [20], and occurs for small

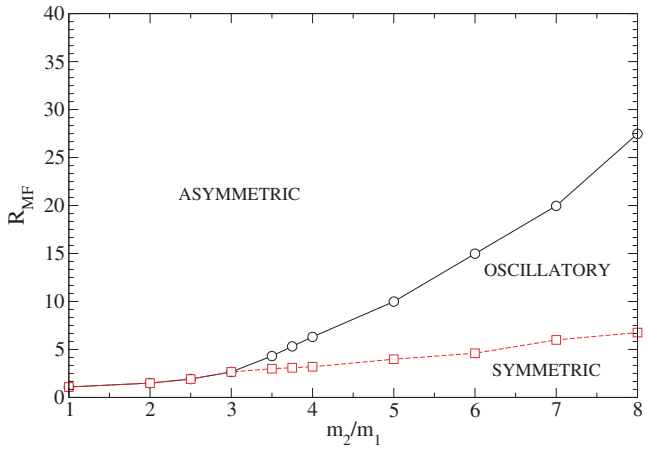

Figure 11. Phase diagram for a system with $N_1 = 70$ light particles and $N_2 = 20$ heavy particles. The transition values of $R_{\rm MF}$ are plotted as functions of the mass ratio m_2/m_1.

mass differences or small concentrations ($m_2/m_1 = 2$, for example). In the second scenario, the temporal evolution of the occupation numbers approaches a limit cycle, so particles of each species oscillate back and forth between compartments. This occurs when the difference in mass is large, or when masses are equal but sizes are different enough [27]. Such a non-steady regime has no counterpart in the case of mono-disperse granular gases. Specifically, when the mass difference between the two species exceeds a certain threshold the populations display a bistable behaviour, with particles of each species switching back and forth between compartments.

Oscillations have their origin in the mass and/or size difference between the two species and in the associated breakdown of energy equipartition that occurs in a binary vibrated granular gas [28–32]. After an initial clustering of both species in a single compartment—say the left—a net rightward flux of light particles establishes and persists until a sufficient number of them have changed compartment. At this point the heavy particles, too, start jumping to the right, eventually creating in the right compartment a cluster of both species which is totally similar to the initial situation of the left compartment. After reaching this stage, the process repeats itself in the opposite direction.

In [22] the mean-field 'phase diagram' of the model was obtained, using as control parameter the variable $R_{\rm MF} \propto (1 - r^2)\frac{N^2}{V^2}\frac{T_s}{T_b}$, which has the property of decreasing for large driving intensities and of increasing when $r \to 0$ and/or the density increases. The resulting 'phase diagram'[2] in the plane $R_{\rm MF}$ versus m_2/m_1 is shown in figure 11. No oscillations can be observed for small mass asymmetry ($\frac{m1}{m2} \simeq 1$), and the crossover from the symmetric phase to the asymmetric phase is similar to what occurs in the case of a one-component system. However, when the mass asymmetry increases ($m_2/m_1 > 3$), an intermediate oscillatory regime appears, and no stationary solution is attained anymore.

The effect of concentration on the appearance of oscillations is instead shown in figure 12. For small concentrations of the heavy species $c = N_2/(N_1 + N_2)$, where N_1 and N_2 are the total number of light particles and heavy particles, respectively, there is a direct crossover, as $R_{\rm MF}$ decreases, from the asymmetric 'phase' to the symmetric 'phase'. When the concentration, c, increases, there appears an island of the oscillating 'phase', which subsequently disappears

[2] As also noticed by Barrat and Trizac the transitions observed are not true phase transitions since they are controlled by the system size. Fluctuations can always bring the system from one of the asymmetric states to the other.

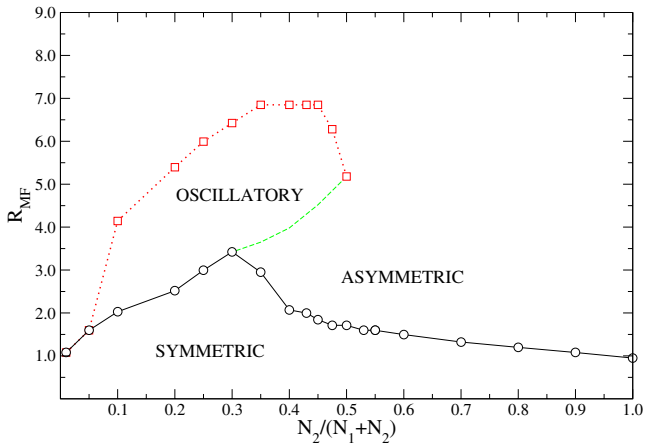

Figure 12. Phase diagram for a system with $N_1 + N_2 = 90$ particles as a function of $N_2/(N_1 + N_2)$, for a mass ratio $m_2/m_1 = 4$.

when c becomes too large. The oscillation period decreases as R_{MF} decreases and is larger near the boundary between the 'broken phase' and the 'oscillatory phase'.

The interesting possibility of separating the two components of the mixture by a similar device has been investigated, but it has been found that the segregation process is not very efficient [29].

6. Numerical studies

The compartmentalized system has attracted attention in recent years and has been the subject of several numerical studies. These studies have been performed by event-driven simulations and direct simulation Monte Carlo (DSMC).

In the DSMC study [20] each particle evolves in time according to an Ornstein–Uhlenbeck process, simulating the interaction with the moving base, and collides inelastically with the remaining particles. In addition, each particle can change compartment with a probability per unit time τ_s^{-1}, provided its energy exceeds the threshold, T_s. Since the algorithm is stochastic, the number of particles and kinetic energies in each compartment are subject to temporal fluctuations around their stationary values. In figure 13 we display the distribution of the occupancy of a compartment for three different values of the driving intensity. Interestingly, the distribution displays a single symmetric peak for strong driving, a pronounced broadening close to the critical driving two sharp and well separated peaks for weak driving.

Whereas the DSMC method is very efficient, it does not allow one to account properly for the mutual strong short-range repulsion between the particles. Such a repulsion can be properly described by means of a molecular dynamics event-driven simulation technique. A few numerical studies have been conducted using such an algorithm (see [22, 27, 29]). Qualitatively the numerical simulation results agree with the mean-field predictions as shown in [22], but the comparison remains difficult at a quantitative level due to the approximations involved in deriving the mean-field theory [22].

7. Related models describing granular gases in compartments

In a recent series of papers, Cecconi *et al* [33] have investigated by means of molecular dynamics and phenomenological arguments the properties a one-dimensional model of a

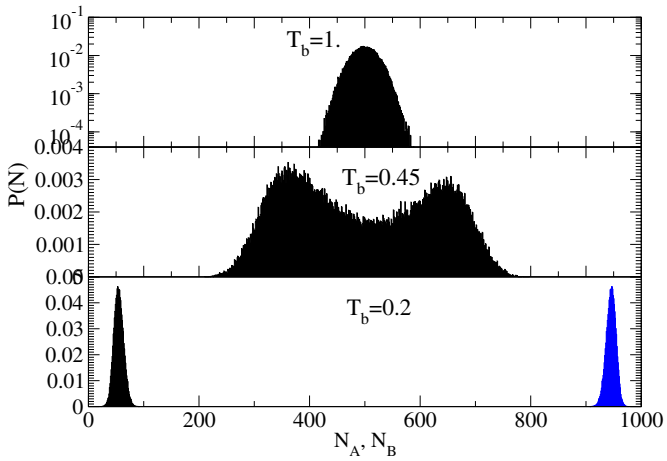

Figure 13. Distribution of occupation numbers for the two-compartment pure model obtained numerically from the DSMC.

compartmentalized system. The advantage of the one-dimensional modelling consists in the fact that it allows an exact treatment of the hard-core interaction and of the spatial gradients at a reasonable computational effort. In addition, theoretical predictions are easier, because the properties of the reference elastic fluid are known. These authors have studied a few relevant situations such as the two-well problem and a periodic array of identical wells. In particular they have derived numerically the shape of the flux function, Φ, for such a model and verified the appearance of a non-monotonic behaviour, as the inelasticity increases. These findings agree with the mean-field analysis reported above.

8. Conclusions

To summarize, we have presented a mean-field description of vibro-fluidized granular matter in compartments. We have derived a Fokker–Planck–Boltzmann description starting from the stochastic evolution of the particle coordinates. Next, by employing a Gaussian ansatz for the velocity distribution function, we have obtained a closed set of equations for the slowly varying fields, namely the granular temperatures and occupation numbers of each compartment. With respect to existing flux models, our approach treats the granular temperature analytically on an equal footing to the occupation variables.

The systems investigated display a rich variety of behaviours which are determined by the inelasticity. For a one-component fluid enclosed in a two-compartment vessel, a mild shaking leads to a symmetry breaking where a dense phase cold 'phase' and a rarefied hot 'phase' coexist. For vigorous shaking, the two 'phases' become identical, and the compartments have the same populations.

The extension to many compartments has been considered, and the main results concern the growth process of the populations in each compartment starting from a uniform distribution. Such a growth resembles in the initial stage the domain growth process following a high-temperature quench in the Cahn–Hilliard model. A measure of the complexity of the profile has been employed in order to characterize the ordering process.

Finally, the theory has been applied to a bi-disperse granular mixture and the observed oscillatory solutions, not present in mono-disperse systems, have also been found in molecular dynamics simulations.

Acknowledgments

UMBM acknowledges the support of the Project Complex Systems and Many-Body Problems Cofin-MIUR 2003 prot 2003020230.

References

[1] Pöschel T and Luding S (ed) 2001 *Granular Gases* (*Springer Lecture Notes in Physics* vol 564) (Berlin: Springer)
[2] Jaeger H M, Nagel S R and Behringer R P 1996 *Rev. Mod. Phys.* **68** 1259 and references therein
[3] Umbanhowar P B, Melo F and Swinney H L 1996 *Nature* **382** 793
[4] Shinbrot T and Muzzio F J 2001 *Nature* **410** 251
[5] Goldhirsch I and Zanetti G 1993 *Phys. Rev. Lett.* **70** 1619
[6] Goldhirsch I, Tan M L and Zanetti G 1993 *J. Sci. Comput.* **8** 1
[7] McNamara S and Young W R 1994 *Phys. Rev.* E **50** R28
[8] Baldassarri A, Marini Bettolo Marconi U and Puglisi A 2002 *Phys. Rev.* E **65** 051301
[9] Schlichting H J and Nordmeier V 1996 *Math. Naturwiss. Unterr.* **49** 323
[10] Eggers J 1999 *Phys. Rev. Lett.* **83** 5322
[11] van der Meer D, van der Weele K and Lohse D 2001 *Phys. Rev.* E **63** 061304
[12] van der Meer D, van der Weele K and Lohse D 2002 *Phys. Rev. Lett.* **88** 174302
[13] van der Weele K, van der Meer D and Lohse D 2001 *Europhys. Lett.* **53** 328
[14] Lipowski A and Droz M 2002 *Phys. Rev.* E **65** 031307
Lipowski A *et al* 2002 *Phys. Rev.* E **66** 016118
Coppex F *et al* 2002 *Phys. Rev.* E **66** 011305
[15] Shim G M, Park B Y, Noh J D and Lee H 2004 *Phys. Rev.* E **70** 031305
[16] Ehrenfest P and Ehrenfest T 1990 *The Conceptual Foundations of the Statistical Approach in Mechanics* (New York: Dover)
Kac M and Logan J 1987 *Fluctuation Phenomena* ed E W Montroll and J L Lebowitz (Amsterdam: North-Holland)
[17] Spitzer F 1970 *Adv. Math.* **5** 246
[18] Evans M R and Hanney T 2005 *Preprint* cond-mat/0501338
[19] Javier Brey J, Moreno F, García-Rojo R and Ruiz-Montero M J 2002 *Phys. Rev.* E **65** 011305
[20] Marini Bettolo Marconi U and Puglisi A 2003 *Phys. Rev.* E **68** 031306
[21] Marini Bettolo Marconi U and Conti M 2004 *Phys. Rev.* E **69** 011302
[22] Costantini G, Cattuto C, Paolotti D and Marini Bettolo Marconi U 2005 *Physica* A **347** 411
[23] The external drive is modeled via a stochastic force. See Puglisi A, Loreto V, Marini Bettolo Marconi U, Petri A and Vulpiani A 1998 *Phys. Rev. Lett.* **81** 3848
Puglisi A, Loreto V, Marini Bettolo Marconi U and Vulpiani A 1999 *Phys. Rev.* E **59** 5582
[24] Van Noije T P C and Ernst M H 1998 *Granular Matter* **1** 57
[25] Cahn J W and Hilliard J E 1958 *J. Chem. Phys.* **28** 258
[26] Mikkelsen R, van der Meer D, van der Weele K and Lohse D 2001 *Phys. Rev. Lett.* **89** 214301
[27] A similar observation was reported by Lambiotte R and Salazar M 2003 *Preprint*
[28] Garzó V and Dufty J W 1999 *Phys. Rev.* E **60** 5706
[29] Barrat A and Trizac E 2003 *Mol. Phys.* **101** 1713
[30] Paolotti D, Cattuto C, Marini Bettolo Marconi U and Puglisi A 2003 *Granular Matter* **5** 75
[31] Pagnani R, Marini Bettolo Marconi U and Puglisi A 2002 *Phys. Rev.* E **66** 051304
Marini Bettolo Marconi U and Puglisi A 2002 *Phys. Rev.* E **66** 011301
[32] Feitosa K and Menon N 2002 *Phys. Rev. Lett.* **88** 198301
[33] Cecconi F, Marini Bettolo Marconi U, Puglisi A and Vulpiani A 2003 *Phys. Rev. Lett.* **90** 064301
Cecconi F, Marini Bettolo Marconi U, Puglisi A and Diotallevi F 2004 *J. Chem. Phys.* **121** 5125
Cecconi F, Marini Bettolo Marconi U, Puglisi A and Diotallevi F 2004 *J. Chem. Phys.* **120** 35